

Dilepton production from SIS to LHC energies

E L Bratkovskaya^{1,2}, O Linnyk³, V P Konchakovski³, W Cassing³,
V Ozvenchuk², J Manninen^{1,2} and C M Ko⁴

¹ Institute for Theoretical Physics, University of Frankfurt, Frankfurt, Germany

² Frankfurt Institute for Advanced Studies, 60438 Frankfurt am Main

³ Institute for Theoretical Physics, University of Giessen, Giessen, Germany

⁴ Texas A& M University, Texas, U.S.A.

E-mail: Elena.Bratkovskaya@th.physik.uni-frankfurt.de

Abstract. We study e^+e^- pair production in proton-proton and in nucleus-nucleus collisions from SIS to LHC energies within the parton-hadron-string dynamics (PHSD) approach which incorporates explicit partonic degrees-of-freedom in terms of strongly interacting quasiparticles (quarks and gluons) in line with an equation-of-state from lattice QCD as well as the dynamical hadronization and hadronic collision dynamics in the final reaction phase. We find a visible in-medium effect in the low mass dilepton sector from dynamical vector-meson spectral functions from SIS to SPS energies whereas at RHIC and LHC energies such medium effects become more moderate. In the intermediate mass regime from 1.1 to 3 GeV pronounced traces of the partonic degrees of freedom are found at SPS and RHIC energies which supersede the hadronic (multi-meson) channels as well as the correlated and uncorrelated semi-leptonic D -meson decays. The dilepton production from the strongly interacting quark gluon plasma (sQGP) becomes already visible at top SPS energies and more pronounced at RHIC and LHC energies.

1. Introduction

Dileptons, i.e. correlated electron and positron pairs, are one of the key observables in ultra-relativistic nuclear collisions experiments since dileptons are emitted during the whole collision evolution and thus one may probe various aspects at different stages of a relativistic nuclear collision by measuring differential dilepton spectra. Another important feature is that the produced leptons interact only electromagnetically and thus interact only very weakly with the strongly interacting partonic or hadronic medium created in the collisions. In another words, e.g. an initial state Drell-Yan-pair from the early stages of the collision is expected to survive the subsequent evolution of the fireball.

An important dilepton observable is the invariant mass spectrum. The mass spectrum can be roughly divided in 3 different regions, in each of which different physics dominates the radiation. In the low mass region ($M_{e^+e^-} < 1$ GeV) the radiation is dominated by the decays of light mesons (consisting of u , d and s (anti)quarks) and especially gives information about in-medium properties of the ρ^0 meson. In the intermediate mass region (1.1 GeV $< M_{e^+e^-} < 3$ GeV) the dominant hadronic contribution to the invariant mass spectrum is obtained from the decays of open charm mesons, while above the J/ψ peak, first open beauty decays and later on initial state Drell-Yan radiation are expected to dominate the dilepton spectrum. On top of the previously mentioned sources, especially in the intermediate mass region, also radiation from the strongly interacting Quark-Gluon-Plasma (sQGP) can give a significant signal [1] as well as some other

more exotic sources like simultaneous interactions of four pions [2, 3],[4, 5]. These partonic and hadronic channels have been studied in detail in Refs. [6, 7] at the top Super-Proton-Synchrotron (SPS) and Relativistic-Heavy-Ion-Collider (RHIC) energies and it has been found that the partonic channels clearly dominate over multi-pion sources in the intermediate dilepton mass regime. This contribution aims to summarize the perspectives of dilepton measurements from low SIS to high LHC energies based on the Parton-Hadron-String Dynamics (PHSD) transport model [8].

2. The PHSD approach

The dynamics of partons, hadrons and strings in relativistic nucleus-nucleus collisions is analyzed here within the Parton-Hadron-String Dynamics approach [8]. In this transport approach the partonic dynamics is based on Kadanoff-Baym equations for Green functions with self-energies from the Dynamical QuasiParticle Model (DQPM) [9] which describes QCD properties in terms of 'resummed' single-particle Green functions. In Ref. [10], the actual three DQPM parameters for the temperature-dependent effective coupling were fitted to the recent lattice QCD results of Ref. [11]. The latter lead to a critical temperature $T_c \approx 160$ MeV which corresponds to a critical energy density of $\epsilon_c \approx 0.5$ GeV/fm³. In PHSD the parton spectral functions ρ_j ($j = q, \bar{q}, g$) are no longer δ -functions in the invariant mass squared as in conventional cascade or transport models but depend on the parton mass and width parameters which were fixed by fitting the lattice QCD results from Ref. [11]. We recall that the DQPM allows one to extract a potential energy density V_p from the space-like part of the energy-momentum tensor as a function of the scalar parton density ρ_s . Derivatives of V_p w.r.t. ρ_s then define a scalar mean-field potential $U_s(\rho_s)$ which enters into the equation of motion for the dynamical partonic quasiparticles. Furthermore, a two-body interaction strength can be extracted from the DQPM as well from the quasiparticle width in line with Ref. [12]. The transition from partonic to hadronic d.o.f. (and vice versa) is described by covariant transition rates for the fusion of quark-antiquark pairs or three quarks (antiquarks), respectively, obeying flavor current-conservation, color neutrality as well as energy-momentum conservation [8, 10]. Since the dynamical quarks and antiquarks become very massive close to the phase transition, the formed resonant prehadronic color-dipole states ($q\bar{q}$ or qqq) are of high invariant mass, too, and sequentially decay to the groundstate meson and baryon octets increasing the total entropy.

On the hadronic side PHSD includes explicitly the baryon octet and decouplet, the 0^- - and 1^- -meson nonets as well as selected higher resonances as in the Hadron-String-Dynamics (HSD) approach [13, 14]. Hadrons of higher masses (> 1.5 GeV in case of baryons and > 1.3 GeV for mesons) are treated as 'strings' (color-dipoles) that decay to the known (low-mass) hadrons, according to the JETSET algorithm [15]. Note that PHSD and HSD merge at low energy density, in particular below the critical energy density $\epsilon_c \approx 0.5$ GeV/fm³. For more detailed descriptions of PHSD and its ingredients we refer the reader to Refs. [9, 10, 16, 17].

The PHSD approach was applied to nucleus-nucleus collisions from $s_{NN}^{1/2} \sim 5$ to 200 GeV in Refs. [8, 10] in order to explore the space-time regions of partonic matter. It was found that even central collisions at the top-SPS energy of $\sqrt{s_{NN}} = 17.3$ GeV show a large fraction of nonpartonic, *i.e.* hadronic or string-like matter, which can be viewed as a hadronic corona. This finding implies that neither hadronic nor only partonic models can be employed to extract physical conclusions in comparing model results with data.

3. Results for dilepton spectra in comparison to experimental data

We directly continue with the results from PHSD in comparison with the available experimental data on dilepton production from SIS to RHIC energies.

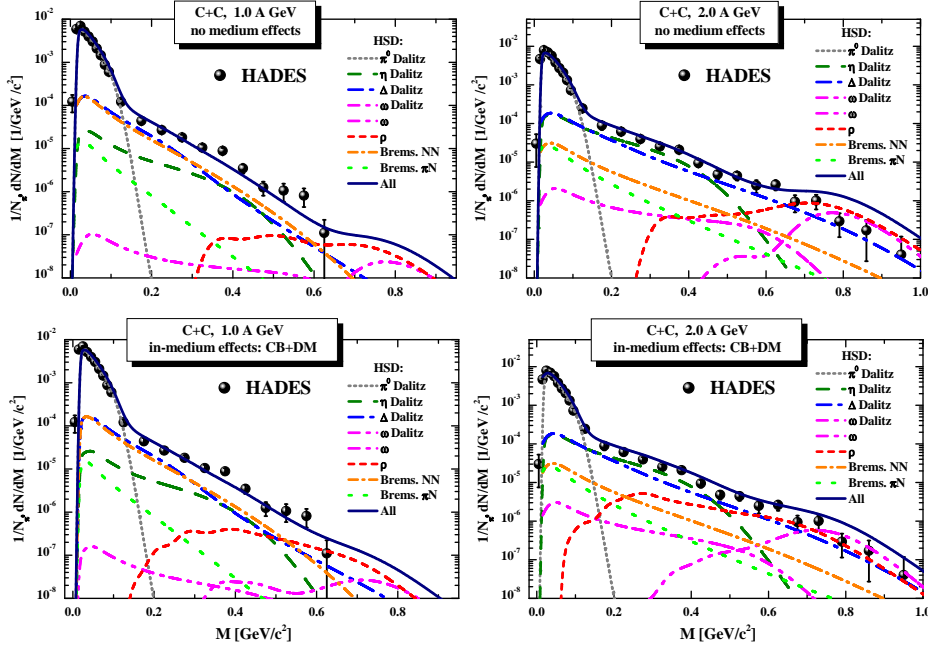


Figure 1. Results of the HSD transport calculation for the mass differential dilepton spectra - divided by the average number of π^0 's - in case of $^{12}\text{C} + ^{12}\text{C}$ at 1.0 A GeV (left) and 2.0 A GeV (right) in comparison to the HADES data [40, 29]. The upper part shows the case of 'free' vector-meson spectral functions while the lower part gives the result for the 'dropping mass + collisional broadening' scenario. In both scenarios the HADES acceptance filter and mass resolution have been incorporated. The different color lines display individual channels in the transport calculation (see legend).

3.1. SIS energies

The dileptons produced in low energy heavy-ion collisions have been measured first by the DLS Collaboration at Berkeley [18, 19, 20, 21]. The observed dilepton yield [21] in the mass range from 0.2 to 0.5 GeV in C+C and Ca+Ca collisions at 1 A GeV was about of five times higher than the calculations by different transport models using the 'conventional' dilepton sources as bremsstrahlung, π^0 , η , ω and Δ Dalitz decays and direct vector mesons (ρ , ω , ϕ) decays [22, 23, 24]. Even after including the different in-medium scenarios as collisional broadening and dropping mass for the ρ -meson spectral function did not solve the 'DLS puzzle' [25, 26, 27, 28].

The recent experimental data from the HADES Collaboration at GSI [29, 30, 31, 32, 33, 34], however, confirmed the measurement of the DLS Collaboration for C+C at 1.0 A GeV [30] as well as for the elementary reactions [35]. In the mean time also the theoretical transport approaches as well as effective models for the elementary NN reactions have been further developed.

A possible solution of the 'DLS puzzle' from the theoretical side has been suggested in Ref. [37] by incorporating stronger pn and pp bremsstrahlung contributions in line with the updated One-Boson-Exchange (OBE) model calculations from Ref. [36]. As shown in Ref. [37] the results of the HSD model (off-shell Hadron-String-Dynamics (HSD) transport approach) with 'enhanced' bremsstrahlung cross sections agree very well with the HADES data for C+C at 1 and 2 A GeV as well as with the DLS data for C + C and Ca + Ca at 1 A GeV, especially when including a collisional broadening in the vector-meson spectral functions. A similar finding has been obtained by other independent transport groups – IQMD [38] and Rossendorf BUU [39].

Fig. 1 shows a comparison of the HSD results to the HADES mass-differential dilepton spectra for C + C at 1.0 A GeV (left) and 2.0 A GeV (right) [40, 29] for the 'free' (upper

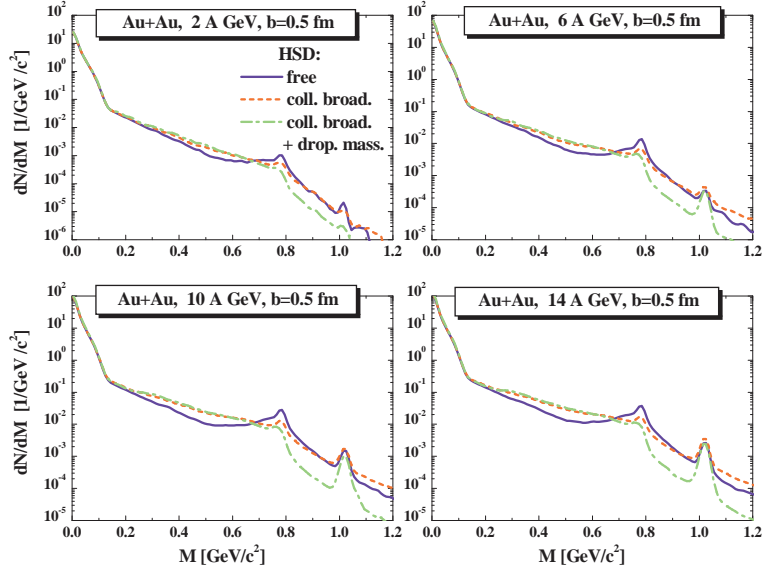


Figure 2. Results of the HSD transport calculation for the mass differential dilepton spectra for central Au+Au collisions from 2 to 14 A GeV calculated for different in-medium scenarios - collisional broadening and combined scenario (dropping mass + collisional broadening).

part) and the in-medium scenario (lower part). At the higher bombarding energy the η Dalitz decay provides the dominant contribution in the mass region from 0.2 to 0.5 GeV followed by Δ Dalitz decays and the combined bremsstrahlung channels. The mass region around 0.75 GeV is overestimated in the 'free' scenario, whereas including in-medium spectral functions for the vector mesons the description of the data is improved due to shifting of the strength from the vector-meson pole mass regime to lower invariant mass. However, the in-medium effects for the light $C + C$ system are only very moderate. In order to observe a strong broadening of the ρ -meson spectral function one has to investigate a larger size system such as $Au + Au$. A corresponding measurement has been performed recently by the HADES Collaboration and the upcoming data will provide more accurate information on the in-medium effects.

In Fig. 2 we show the HSD predictions for the dilepton yields from central Au + Au collisions calculated for different energies from 2 to 14 A GeV applying the different in-medium scenarios: collisional broadening and combined approach (dropping mass + collisional broadening). One can see that both scenarios lead to an enhancement of the dilepton yield in the mass region $M = 0.3 - 0.8$ GeV by a factor of about 2. The largest in-medium effect is, however, attributed to the reduction of the dilepton yield between the ω and ϕ peaks due to the downward shift of the poles of the ρ and ω spectral functions. However, the latest scenario is not consistent with existing experimental data at higher energies, so one has to rely most likely on the relatively modest in-medium effects due to collisional broadening.

3.2. SPS energies

We step up in energy and compare our model results with experimental data for dileptons from In+In collisions at 160 A GeV measured by the NA60 Collaboration.

In Fig. 3 we present PHSD results for the dilepton excess over the known hadronic sources as produced in In+In reactions at 158 A GeV compared to the acceptance corrected data. We find here that the spectrum at invariant masses in the vicinity of the ρ peak is well reproduced by the ρ meson yield, if a broadening of the meson spectral function in the medium is assumed, while the partonic sources account for the yield at high masses. Our analysis shows that the

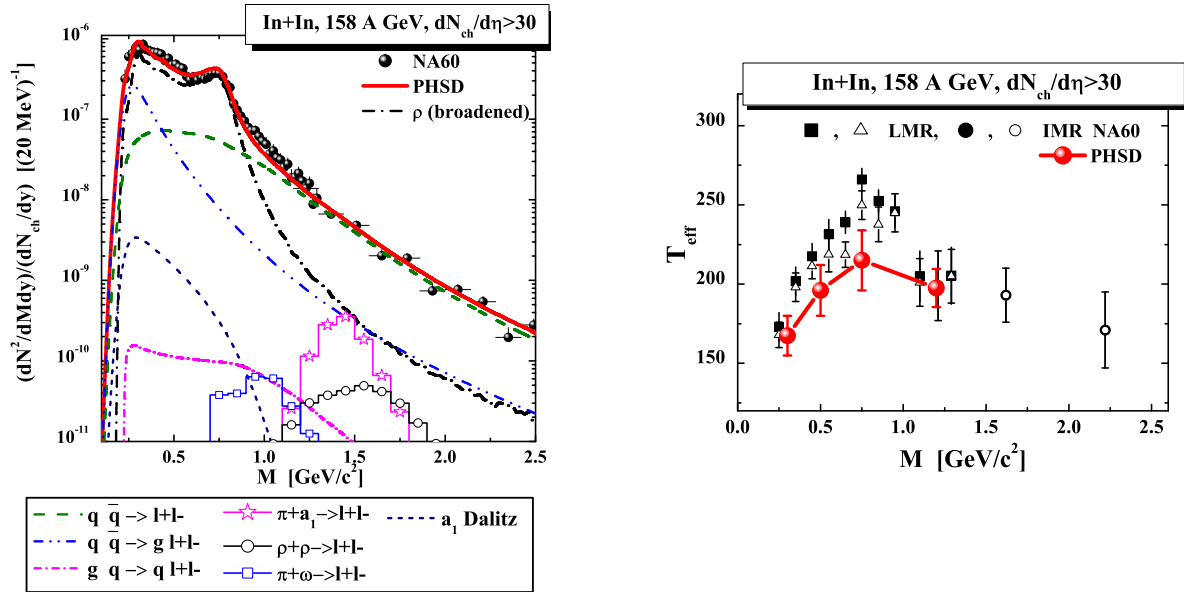


Figure 3. Left: Acceptance corrected mass spectra of excess dimuons from In+In at 158 A GeV integrated over p_T in $0.2 < p_T < 2.4$ GeV from PHSD compared to the data of NA60 [41]. The dash-dotted line shows the dilepton yield from the in-medium ρ with a broadened spectral function, the dashed line presents the yield from the $q + \bar{q}$ annihilation, the dash-dot-dot line gives the contribution of the gluon Bremsstrahlung process ($q\bar{q} \rightarrow gl^+l^-$), while the solid line is the sum of all contributions. For the description of the other lines, which correspond to the non-dominant channels, we refer to the figure legend. Right: The inverse slope parameter T_{eff} of the dimuon yield from In+In at 158 A GeV as a function of the dimuon invariant mass in PHSD compared to the data of the NA60 Collaboration [42, 41].

contributions of the ‘ 4π ’ processes (shown by the lines with symbols), first noted by the authors of Ref. [2], are very much suppressed.

One concludes from Fig. 3 that the measured spectrum for $M > 1$ GeV is dominated by the *partonic* sources. Indeed, the domination of the radiation from the QGP over the hadronic sources in PHSD is related to a rather long – of the order of 3 fm/c – evolution in the partonic phase (in co-existence with the space-time separated hadronic phase) on one hand (cf. Fig. 10 of Ref. [43]) and the rather high initial energy densities created in the collision on the other hand (cf. Fig. 6 of Ref. [44]). In addition, we find from Fig. 3 that in PHSD the partonic sources also have a considerable contribution to the dilepton yield for $M < 0.6$ GeV. The yield from the two-to-two process $q + \bar{q} \rightarrow g + l^+l^-$ is especially important close to the threshold (≈ 0.211 GeV). This conclusion from the microscopic calculation is in qualitative agreement with the findings of an early (more schematic) investigation in Ref.[45].

The comparison of the mass dependence of the slope parameter evolution in PHSD and the data is shown explicitly in the right part of Fig. 3. Including partonic dilepton sources allows us to reproduce in PHSD the m_T -spectra as well as the finding of the NA60 Collaboration [41, 42] that the effective temperature of the dileptons (slope parameters) in the intermediate mass range is lower than that of the dileptons in the mass bin $0.6 < M < 1$ GeV, which is dominated by hadronic sources (cf. Fig. 3, right). The softening of the transverse mass spectrum with growing invariant mass implies that the partonic channels occur dominantly before the collective radial flow has developed. Also, the fact that the slope in the lowest mass bin and the highest one are approximately equal – both in the data and in PHSD – can be traced back to the two

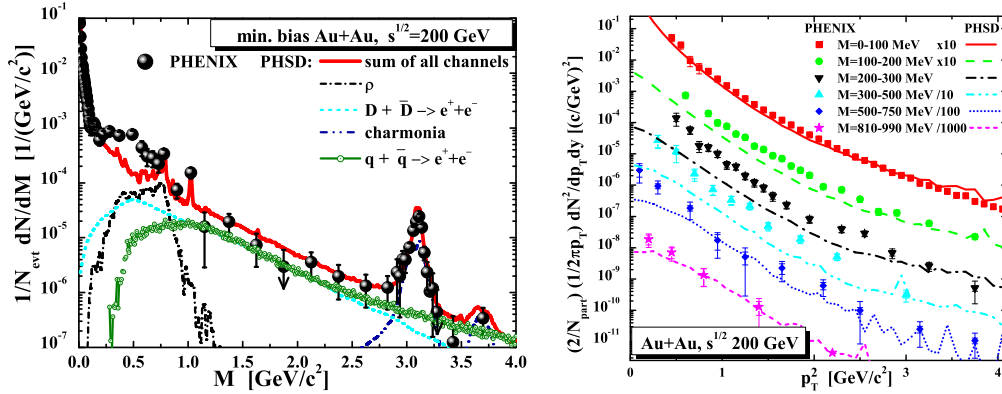


Figure 4. Left: The PHSD results for the invariant mass spectra of inclusive dileptons in Au+Au collisions at $\sqrt{s_{NN}} = 200$ GeV within the PHENIX acceptance cuts in comparison to the data from the PHENIX Collaboration [46, 47]. The different lines indicate the contributions from different channels as specified in the figure. Right: The PHSD results for the transverse-momentum spectra of dileptons from minimum bias Au+Au collisions at $\sqrt{s_{NN}} = 200$ GeV in different mass bins compared to the data from the PHENIX Collaboration [46, 47].

windows of the mass spectrum that in our picture are influenced by the radiation from the sQGP: $M = 2M_\mu - 0.6$ GeV and $M > 1$ GeV. For more details we refer the reader to Ref. [7].

3.3. RHIC energies

Now we are coming to the top RHIC energy of $\sqrt{s_{NN}} = 200$ GeV and present the most important findings from the PHSD study in Ref. [6]. In the left part of Fig. 4 we show our results for the invariant mass spectra of inclusive dileptons in Au+Au collisions for the acceptance cuts on single electron transverse momenta p_{eT} , pseudorapidities η_e , azimuthal angle ϕ_e , and dilepton pair rapidity y : $p_{eT} > 0.2$ GeV, $|\eta_e| < 0.35$, $-3\pi/16 < \phi_e < 5\pi/16$, $11\pi/16 < \phi_e < 19\pi/16$, $|y| < 0.35$.

In the low mass region $M = 0 - 1.2$ GeV, the dilepton yield in the PHSD is dominated by hadronic sources and essentially coincides with the earlier HSD result [48]. Note that the collisional broadening scenario for the modification of the ρ -meson was used in the calculations presented in Fig. 4 that underestimates the PHENIX data from 0.2 to 0.7 GeV substantially. In contrast, the partonic radiation as well as the yield from correlated D -meson decays are dominant in the mass region $M = 1 - 3$ GeV as seen in Fig. 4 (left), i.e. in the mass region between the ϕ and J/Ψ peaks. The dileptons generated by the quark-antiquark annihilation in the sQGP constitute about half of the observed yield in this intermediate-mass range. For $M > 2.5$ GeV the partonic yield even dominates over the D -meson contribution. Thus, the inclusion of the partonic radiation in the PHSD fills up the gap between the hadronic model results [48, 49] and the data of the PHENIX Collaboration for $M > 1$ GeV, however, the early expectation of a partonic signal in the low mass dilepton spectrum is not verified by the microscopic PHSD calculations.

In order to investigate the momentum dependence of the "missing low mass yield", we have calculated the p_T -spectra of dileptons in different bins of invariant mass M . In the right part of Fig. 4 we show the measured transverse momentum spectra of dileptons for minimum bias Au+Au collisions at $\sqrt{s_{NN}} = 200$ GeV (symbols) in comparison with the spectra from the PHSD (lines) for six mass bins as indicated in the figure. Whereas the PHSD can well describe the dilepton spectra in the mass intervals $[0, 100$ MeV] and $[810$ MeV, 990 MeV], it underestimates the low p_T dileptons in the other mass bins, particularly in the mass bins $[300$ MeV, 500 MeV].

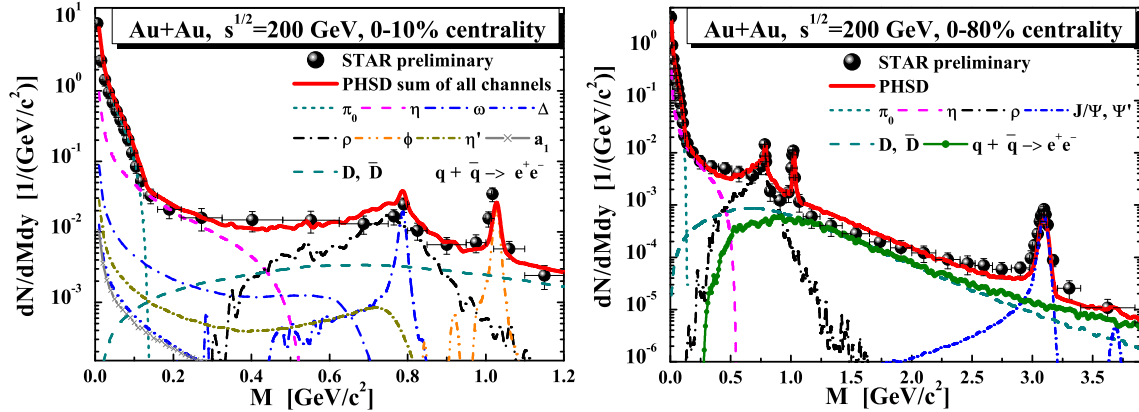


Figure 5. The PHSD results for the invariant mass spectra of dileptons in Au+Au collisions at $\sqrt{s_{NN}} = 200$ GeV for $M=0-1.2$ GeV (left part) and for $M=0-4$ GeV (right part) and 0-10% centrality within the cuts of the STAR experiment. The preliminary data from the STAR Collaboration are adopted from Ref. [50].

On the other hand, high p_T dileptons are reproduced quite well by the PHSD calculations. We conclude that the missing dilepton yield for masses from 0.15 to 0.6 GeV is essentially due to a severe underestimation of the data at low p_T by up to an order of magnitude. We recall that at top SPS energies the low p_T dilepton yield could be attributed to $\pi\pi$ annihilation channels, i.e. to the soft hadronic reactions in the expansion phase of the system. These channels are, however, insufficient to describe the very low slope of the p_T spectra at the top RHIC energy.

In order to shed some light on the 'PHENIX puzzle' we step to a comparison of the PHSD predictions with the preliminary STAR data measured for Au+Au collisions at $\sqrt{s_{NN}} = 200$ GeV with the acceptance cuts on single electron transverse momenta p_{eT} , single electron pseudorapidities η_e and the dilepton pair rapidity y , i.e. $0.2 < p_{eT} < 5$ GeV, $|\eta_e| < 1$, $|y| < 1$. Our predictions for the dilepton yield within these cuts are shown in Fig. 5 for 0-80% centrality. One can observe generally a good agreement with the preliminary data from the STAR Collaboration [50] in the whole mass regime. Surprisingly, our calculations are also roughly in line with the low mass dilepton spectrum from STAR in case of central collisions whereas the PHSD results severely underestimate the PHENIX data for central collisions. The observed dilepton yield from STAR at masses below 1.2 GeV can be accounted for by the known hadronic sources, i.e. the decays of the π_0 , η , η' , ω , ρ , ϕ and a_1 mesons, of the Δ particle and the semileptonic decays of the D and \bar{D} mesons, where the collisional broadening of the ρ meson is taken into account.

The discrepancy between the PHENIX and STAR data will have to be investigated closer by the experimental collaborations. Furthermore, the upgrade of the PHENIX experiment with a hadron blind detector should provide decisive information on the origin of the low mass dileptons produced in the heavy-ion collisions at $\sqrt{s_{NN}} = 200$ GeV.

4. Conclusions

We close this contribution by noting that the dileptons are an interesting probe of the dynamical processes in heavy-ion collisions at all energy regimes. The low-mass dileptons provide information on the vector meson spectral function in the medium whereas the high mass part from 1.1 to 3 GeV can be attributed dominantly to the partonic annihilation in the QGP phase. At the higher RHIC and LHC energies the modifications of the low-mass sector are less pronounced than at SIS and SPS energies, however, the dilepton emissivity from the sQGP

becomes substantial or even dominant relative to the background from D -meson decays.

The authors acknowledge the financial support through the “HIC for FAIR” framework of the “LOEWE” program and the Deutsche Forschungsgemeinschaft (DFG).

References

- [1] Shuryak E V 1978 *Phys. Lett. B* **78** 150; 1978 *Sov. J. Nucl. Phys.* **28** 408; 1978 *Yad.Fiz.* **28** 796.
- [2] Song C, Ko C M and Gale C 1994 *Phys. Rev. D* **50** 1827
- [3] Li G Q and Gale C 1998 *Phys. Rev. C* **58** 2914 [arXiv:nucl-th/9807005].
- [4] van Hees H and Rapp R 2006 *Phys. Rev. Lett.* **97** 102301
- [5] van Hees H and Rapp R 2008 *Nucl. Phys. A* **806** 339
- [6] Linnyk O, Cassing W, Manninen J, Bratkovskaya E L and Ko C M 2012 *Phys. Rev. C* **85** 024910
- [7] Linnyk O, Bratkovskaya E L, Ozvenchuk V, Cassing W and Ko C M 2011 *Phys. Rev. C* **84** 054917
- [8] Cassing W and Bratkovskaya E L 2009 *Nucl. Phys. A* **831** 215
- [9] Cassing W 2007 *Nucl. Phys. A* **795** 70
- [10] Bratkovskaya E L, Cassing W, Konchakovski V P and Linnyk O 2011 *Nucl. Phys. A* **856** 162
- [11] Aoki Y *et al.* 2009 *JHEP* **0906** 088
- [12] Peshier A and Cassing W 2005 *Phys. Rev. Lett.* **94** 172301
- [13] Ehehalt W and Cassing W 1996 *Nucl. Phys. A* **602** 449
- [14] Cassing W and Bratkovskaya E L 1999 *Phys. Rep.* **308** 65
- [15] Bengtsson H U and Sjöstrand T 1987 *Comp. Phys. Commun.* **46** 43
- [16] Cassing W 2007 *Nucl. Phys. A* **791** 365
- [17] Cassing W 2009 *Eur. J. Phys.* **168** 3
- [18] Matis H S *et al.*, DLS Collaboration 1995 *Nucl. Phys. A* **583** 617C
- [19] Wilson W K *et al.* DLS Collaboration 1998 *Phys. Rev. C* **57** 1865
- [20] Wilson W K *et al.* DLS Collaboration 1993 *Phys. Lett. B* **316** 245
- [21] Porter R J *et al.* DLS Collaboration 1997 *Phys. Rev. Lett.* **79** 1229
- [22] Wolf G, Cassing W and Mosel U 1993 *Prog. Part. Nucl. Phys.* **30** 273
- [23] Bratkovskaya E L, Cassing W and Mosel U 1996 *Phys. Lett. B* **376** 12
- [24] Xiong L, Wu Z G, Ko C M and Wu J Q 1990 *Nucl. Phys. A* **512** 772
- [25] Ernst C, Bass S A, Belkacem M, Stoecker H and Greiner W 1998 *Phys. Rev. C* **58** 447
- [26] Bratkovskaya E L, Cassing W, Rapp R, and Wambach J 1998 *Nucl. Phys. A* **634** 168
- [27] Bratkovskaya E L and Ko C M *Phys. Lett. B* **445** 265
- [28] Fuchs C, Faessler A, Cozma D, Martemyanov B V and Krivoruchenko M I 2005 *Nucl. Phys. A* **755** 499
- [29] Agakishiev G *et al.*, HADES Collaboration 2008 *Phys. Lett. B* 663 43
- [30] Pachmayer Y C *et al.*, HADES Collaboration 2008 *J. Phys. G* **35** 104159
- [31] Sudol M *et al.*, HADES Collaboration 2009 *Eur. Phys. J. C* **62** 81
- [32] Agakishiev G *et al.*, HADES Collaboration 2010 *Phys. Lett. B* **690** 118
- [33] Lapidus K *et al.*, HADES Collaboration arXiv:0904.1128 [nucl-ex].
- [34] Agakishiev G *et al.*, HADES Collaboration 2011 *Phys. Rev. C* **84** 014902
- [35] Agakishiev G *et al.*, HADES Collaboration, 2012 *Phys. Rev. C*, in press, arXiv1203.2549 [nucl-ex]
- [36] Kaptari L P and Kämpfer B 2006 *Nucl. Phys. A* **764** 338
- [37] Bratkovskaya E L and Cassing W, 2008 *Nucl. Phys. A* **807** 214
- [38] Thomere M, Hartnack C, Wolf G and Aichelin J 2007 *Phys. Rev. C* **75** 064902
- [39] Barz H W, Kämpfer B, Wolf G and Zetenyi M arXiv:0910.1541 [nucl-th].
- [40] Agakishiev G *et al.*, HADES Collaboration 2007 *Phys. Rev. Lett.* **98** 052302
- [41] Arnaldi R *et al.*, NA60 Collaboration 2009 *Eur. Phys. J. C* **59** 607
- [42] Arnaldi R *et al.*, NA60 Collaboration 2006 *Phys. Rev. Lett.* **96** 162302; Seixas J *et al.*, 2007 *J. Phys. G* **34** S1023; Damjanovic S *et al.*, 2007 *Nucl. Phys. A* **783**, 327c; Arnaldi R *et al.*, 2009 *Eur. Phys. J. C* **61** 711
- [43] Cassing W and Bratkovskaya E L 2009 *Nucl. Phys. A* **831** 215
- [44] Linnyk O, Bratkovskaya E L, and Cassing W 2008 *Int. J. Mod. Phys. E* **17** 1367
- [45] Alam J, Hirano T, Nayak J K, and Sinha B arXiv:0902.0446.
- [46] Toia A. *et al.*, PHENIX Collaboration, 2006 *Nucl. Phys. A* **774** 743
- [47] Adare A. *et al.*, PHENIX Collaboration 2010 *Phys. Rev. C* **81** 034911
- [48] Bratkovskaya E L, Cassing W and Linnyk O 2009 *Phys. Lett. B* **670** 428
- [49] Manninen J, Bratkovskaya E L, Cassing W and Linnyk O 2011 *Eur. Phys. J. C* **71** 1615
- [50] Zhao J *et al.*, STAR Collaboration arXiv:1106.6146[nucl-ex].